

Asymmetry Analysis of Bilateral Shapes

Kanti V. Mardia^{1,**}, Xiangyu Wu^{1,*}, John T. Kent^{1,*}, Colin R. Goodall^{1,*},

Balvinder S. Khambay^{2,*}

¹Department of Statistics, School of Mathematics, University of Leeds, LS2 9JT, England.

²Third Orthodontics Division, Dentistry, School of Health Sciences, College of Medicine and Health, University of

Birmingham, England.

**Email: k.v.mardia@leeds.ac.uk.

January 21, 2026

Abstract

Many biological objects possess bilateral symmetry with some noise about a midline or midplane. This paper uses landmark-based methods to measure departures from bilateral symmetry, especially for paired data and two-group problems where one group may be more symmetric than the other. We formulate our work under size-and-shape analysis framework including pre-registration under rigid body motion. We then construct a vector of elementary asymmetry features defined per landmark coordinate per object. Next, we introduce two approaches for comparing bilateral symmetry between the two groups or paired data: (1) the elementary features are combined into a scalar asymmetry measure for each object, then standard univariate tests are used to test for asymmetries; (2) a univariate test statistic is constructed for each feature, then the maximum of these statistics leads to an overall test statistic and important features can be extracted from the data. Our methodology is illustrated on two registered datasets collected to assess the success of two kinds of surgeries:

(1) cleft lip surgery data, where the symmetry is compared between a group of cleft lip subjects and normal subjects; (2) orthognathic surgery data, where the patients' symmetry after the orthognathic surgery are compared to that before surgery.

Keywords: asymmetry measures, cleft lip surgery, orthognathic surgery, registration, shape analysis, size-and-shape analysis of smile.

1 Introduction

Bilateral symmetry, also called left-right symmetry, is a key property in many biological settings. An object is said to be bilaterally symmetric if its reflection through some midline (for objects in two dimensions) or midplane (for objects in three dimensions) passing through the center of the object is exactly the same as the original object. In practice, exact bilateral symmetry seldom holds and it is of interest to study the extent of any asymmetry. Research on the symmetries of objects in the real world has a long history (see, for example, Weyl, 1952). Statistical methods to test asymmetry were first formalized in Mardia et al. (2000). Subsequently, a wide variety of statistical methods have been developed; see, for examples, Kent and Mardia (2001), Bock and Bowman (2006), Ajmera et al. (2022) and Ajmera et al. (2023).

The focus of this paper is on landmark-based objects as in Mardia et al. (2000). Each object is a set of K labelled points or landmarks, represented as a $K \times M$ configuration matrix giving the positions of K landmarks in M dimensions. The cases $M = 2$ and $M = 3$ are the most important in practice. We call an object *bilateral* if its landmarks can be divided into two categories: *pairs* and *solos*. An object is *bilaterally symmetric* about an $M - 1$ -dimensional midplane \mathcal{P} if all the solos lie on the midplane, and the two landmarks in each pair are equally spaced about \mathcal{P} , meaning that their midpoint lies on \mathcal{P} and the vectors to each from their midpoint are orthogonal to \mathcal{P} . Let there be K_P pairs and K_S solos; then $K = 2K_P + K_S$. After we have determined the M orthogonal axes for the object, the intersection point between the midplane and the first coordinate axis can be computed. Under translation and rotation it is ensured that the midplane \mathcal{P} passes through the origin and is orthogonal to the first coordinate axis. All objects in the dataset should

be registered so that all of them share the same midplane \mathcal{P} , hence, further analyses are available. If the dataset has not been pre-registered before the analyses, then registration is required; the details are given in Section 2.1.

This paper is motivated by two medical questions related to the level of asymmetry in a person's smile. One is related to cleft lip surgery which is performed so that form and function can be restored to particularly lip symmetry at rest and during movement. The second is related to orthognathic surgery, which is performed to correct jaw discrepancies in order to restore the form and function but the surgery can influence facial and lip symmetry.

We have been provided with appropriate data in each case. We will refer the cleft lip data as Smile Data 1, and the orthognathic surgery data as Smile Data 2. In both datasets, we have a set of landmarks on the lip area as appropriate to each case; Smile Data 1 contains 24 landmarks over the lip while Smile Data 2 contains 16 landmarks over the lip and nose. More details of the data are provided in Section 5 and Section 6 respectively. In each case, the subjects were asked to smile from rest (close lip) to maximum open lip smile and a four-dimensional (three spatial dimensions plus time) movie capture was made of the face using Di4D motion capture system (<https://di4d.com>). A superimposed finite element mesh combined with optical flow techniques were used to follow the landmarks through the frames of the capture, taken at one-second intervals, of the capture. Note that these include both anatomical landmarks, e.g. the corners of the mouth, and pseudo landmarks, e.g. a midpoint of the upper right lip defined at first frame and then followed through successive frames of the capture by optical flow.

Smile Data 1 contains two groups: normal subjects and subjects who had previous cleft lip surgery. Smile Data 2 includes a single group of subjects before and after orthognathic surgery, so it is a paired dataset. The aim is to assess the success of these two different surgeries, that is, are the cleft lip subjects more symmetric after the surgery, and has orthognathic surgery had an impact on symmetry. Both datasets are pre-registered in the same way and we have three fixed frames (the beginning, middle and end of the smile) for each subject.

The asymmetry information in an object is represented as a vector of *coordinatewise elementary*

asymmetry features, \mathbf{d} , say, defined in Section 2.2. Increasing the magnitude of any element in \mathbf{d} indicates greater asymmetry. The elementary feature vector is also the starting point of Bock and Bowman (2006) and Patel et al. (2023), and we define its elements explicitly in Section 2.2.

Given two groups of objects, a natural question is whether one group is more asymmetric than the other. Section 3 looks at two testing strategies which we name combine-then-compare and compare-then-combine respectively.

Our methodology involves simultaneous comparisons, hence, meta-analysis is considered. The literature on meta-analysis as required in the paper is scattered over several papers, and in Section 4, we give an overview of meta-analysis as required for our work. The meta-analysis is carried out in Section 5 and 6 respectively for the two datasets.

The paper concludes with a discussion in Section 7.

2 Describing asymmetry

2.1 Registration

We introduce the following notations: let X , with elements $X[k, m]$, be a $K \times M$ configuration matrix giving the positions of K landmarks in M dimensions for a single object or subject or individual, where $k = 1, \dots, K$ and $m = 1, \dots, M$. We write as $X[k,] \in \mathbb{R}^M$ for the coordinates of the k th landmark, $k = 1, \dots, K$. The most important choice is $M = 3$, and this case is emphasized in the presentation, but the mathematical theory is valid for any dimension $M \geq 1$. In general, upper case letters are used for matrices and bold lower case letters for vectors. In addition the letters K, M, J are reserved for the number of landmarks, number of dimensions, and number of elementary features (Section 2.2), respectively, with typical indices given by the lower case letters k, m, j . In general, each data object X will be viewed as a noisy version of a bilaterally symmetric configuration X^S .

Rigid body transformations If X is a configuration, then a *rigid body motion* takes X to $X^* = \mathbf{1}_M \mathbf{c}^T + XR$, say, where $\mathbf{c} \in \mathbb{R}^M$ is a translation vector and R is an $M \times M$ rotation

matrix. For the purposes of this paper, we say that X and X^* have the same *size-and-shape*, as the size-and-shape of X is the equivalence class of configurations under the group of rigid body motions (see, for example, Dryden and Mardia (2016)). The asymmetry information carried by the size-and-shape is of interest and such information is unaffected under rigid body motion. The size is emphasized here, since the size information is taken into consideration. Recall that the term “shape” is a standard terminology in statistical shape analysis which means the equivalence class under the larger group of similarity transformations so the scale is also filtered out.

A hyperplane \mathcal{P} in \mathbb{R}^M can be written in the form $\mathcal{P} = \{\mathbf{x} \in \mathbb{R}^M : \mathbf{n}^T \mathbf{x} = b\}$, in terms of a unit normal vector \mathbf{n} , say, and a scalar offset term b , say. When $M = 3$ a hyperplane becomes a two-dimensional plane, and when $M = 2$ a hyperplane becomes a one-dimensional line. For simplicity we refer to hyperplanes as planes everywhere. Under a rigid body motion, \mathbf{n} is transformed to $R^T \mathbf{n}$ and b is transformed to $b + \mathbf{n}^T R \mathbf{c}$.

Two types of Registration We distinguish two types of registrations

- (a) Axis registration.
- (b) Basis registration.

Suppose there is an associated midplane \mathcal{P} for every bilateral data object X . Ways in which \mathcal{P} might be determined are discussed below. For data analysis, it is helpful to “register” X using a rigid body motion so that after transformation $\mathbf{n} = \mathbf{e}_1$ and $b = 0$, i.e., the midplane passes through the origin and the normal direction is given by the first coordinate axis, while still keeps the size-and-shape of X unchanged.

In some settings it is possible to carry out a stronger version of registration than the axis registration, we will call *basis registration*, in which all the coordinate axes have a natural interpretation. In our illustrative smile examples, for 3D measurements of the human head, the midplane is known as the sagittal plane, and it is natural to require the coordinate axes to have the following interpretations:

- (a) x -coordinate: left-right

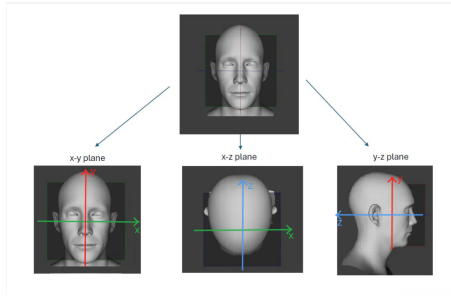


Figure 1: Coordinates system used for registration of human face used in our illustrative smile examples: with three principal planes. In the figure at top row, the x - y plane is in green, the y - z plane is in red and the x - z plane is in blue. For the three sub-figures in the bottom row, the x -axis is in green, y -axis is in red and z -axis is in blue.

(b) y -coordinate: down-up

(c) z -coordinate: back-front

Figure 1 shows these coordinate axes as well as the three planes on a human face which have been used in pre-registration for our smile data. That is, the x -axis is positioned horizontally on the face (positive direction is left from the view point of the subject), the y -axis is placed vertically on the face (positive direction is upward), whereas the z -axis is positioned in the direction inwards and outwards of the face (positive direction is outward), see Figure 1.

In general, to carry out basis registration, it is also necessary to know or estimate $M - 1$ meaningful basis vectors in \mathcal{P} . In this case the three possibilities become: (a) the basis is known a priori; (b) the basis is estimated using expert knowledge; or (c) the basis is estimated using hybrid Procrustes analysis. For details of Procrustes analysis, see, for example, Goodall (1991) and Dryden and Mardia (2016).

For our illustrative smile examples, expert knowledge (scenario (b)) has been used to estimate the midplane with the stated interpretations for the coordinate axes as above (Figure 1). It may be noted that there will be one more reflection before the registration in some data; specifically, for those cleft lip subjects in Smile Data 1 with the cleft on the right, we reflect in the midplane so that the cleft is consistently on the left.

2.2 Elementary features

Suppose the size-and-shape dataset has been basis registered about a midplane \mathcal{P} that passes through the origin and is normal to the first coordinate axis and the $M - 1$ axes of \mathcal{P} are all determined. Then it is possible to define various elementary features to describe the asymmetry of each data object. Paired and solo landmarks are treated separately. We begin with an idealized bilaterally symmetric object X^S . Each of the K landmarks of X^S will be either to the left of \mathcal{P} , to the right of \mathcal{P} , or on \mathcal{P} . The counts of landmarks in these subsets are respectively K_L , K_R , and K_S where $K_L = K_R = K_P$.

For any $K \times M$ observation X modeled on X^S , landmarks, identified by their indices, follow the prescription of X^S . Let k_L and k_R denote the left and right indices for a typical landmark pair from a bilateral object X and consider the M *coordinatewise signed elementary features* for the landmark pairs,

$$d[(k_L, k_R), 1] = X[k_L, 1] + X[k_R, 1] \quad (2.1)$$

$$d[(k_L, k_R), m] = X[k_L, m] - X[k_R, m], \quad m = 2, \dots, M. \quad (2.2)$$

That is, there is one feature for each coordinate of each landmark pair, so there are in total MK_P coordinatewise features. The first coordinates for the two landmarks in one pair have opposite signs, while other coordinates have the same sign with respect to \mathcal{P} . Note that this pattern is true for both axis and basis registrations. For X^S , the quantities in equations (2.1) and (2.2) should all be 0. Thus, the quantities given in (2.1) and (2.2) quantify the departure from symmetry. Similarly, if k_S is a typical solo landmark, consider the single elementary feature

$$d[(k_S)] = X[k_S, 1]. \quad (2.3)$$

There are in total K_S elementary features for solos. For X^S , the first coordinate of a solo landmark will be 0, with no restriction on other coordinates. Hence, a single feature as in (2.3) is adequate

to describe the asymmetry of a solo landmark.

The coordinatewise elementary features can be collected into a *signed elementary feature vector* $\mathbf{d} = (d_j)$, say, of length $J_{\text{basis}} = MK_P + K_S$. The elements of \mathbf{d} will either be listed sequentially with a subscript index, i.e., d_j , $j = 1, \dots, J_{\text{basis}}$, or using parentheses within square brackets, as in (2.1)-(2.3). Note that the vector \mathbf{d} is a function of matrix X and \mathcal{P} .

When only axis registration is available, the coordinate information in (2.2) does not have a well-defined interpretation. This is because the coordinates except the first one of paired landmarks would be changed after rotation within \mathcal{P} , hence leads to changes in values of (2.2) even though the asymmetry information does not change (but note that equation (2.1) does not change). Further, at each landmark the coordinate information can be collected into a single number, called a *landmark elementary feature* which is defined per landmark,

$$d^*[(k_L, k_R)] = \left\{ \sum_{m=1}^M d^2[(k_L, k_R), m] \right\}^{1/2}, \quad d^*[(k_S)] = |X[k_S, 1]|, \quad (2.4)$$

where d 's are defined by (2.1) and (2.2).

Another useful way to think about the elementary features is by using reflection. Let $X^{(\text{refl})}$ denote the reflection of X about \mathcal{P} . Computationally, this matrix is obtained by changing the sign of the first column of X and interchanging the row indices for each landmark pair. Then the elementary features of X can be obtained by comparing the elements of X and $X^{(\text{refl})}$. If X is bilaterally symmetric about \mathcal{P} , then $X = X^{(\text{refl})}$ and $\mathbf{d} = \mathbf{0}$.

In many examples, such as the illustrative smile examples studied later in this paper in Section 5 and 6, the direction of asymmetry, for example, left or right asymmetry, can vary between individuals and is not thought interesting. We will focus on the absolute values of the elementary features. Define the *absolute elementary feature vector* \mathbf{a} with elements

$$a_j = |d_j|, \quad j = 1, \dots, J, \quad (2.5)$$

where $J = J_{\text{basis}}$ or $J = J_{\text{axis}}$, as appropriate. In other words, only the extent of the asymmetry is

interesting. The elements of \mathbf{a} can also be written in a similar way as elements of \mathbf{d} in (2.1)-(2.4). In the rest of the paper, each configuration X is reduced to an absolute elementary feature vector \mathbf{a} for further numerical and statistical analysis. Note that \mathbf{a} is also a function of matrix X and \mathcal{P} .

2.3 Example 1

We give here a simple example to illustrate our basic notation and construction of the vector \mathbf{a} and related quantities. Consider two configurations in $M = 2$ dimensions with $K = 4$ landmarks given by

$$X_1 = \begin{pmatrix} X_1[1,]^T \\ X_1[2,]^T \\ X_1[3,]^T \\ X_1[4,]^T \end{pmatrix} = \begin{pmatrix} -1 & 0 \\ 0 & 1 \\ 1 & 0 \\ 0 & -1 \end{pmatrix}, \quad X_2 = \begin{pmatrix} X_2[1,]^T \\ X_2[2,]^T \\ X_2[3,]^T \\ X_2[4,]^T \end{pmatrix} = \begin{pmatrix} -0.95 & 0.36 \\ -0.28 & 2.11 \\ 0.99 & 0.54 \\ -0.31 & -1.37 \end{pmatrix}. \quad (2.6)$$

Therefore, there is one landmark pair $(k_L, k_R) = (1, 3)$ and two solos, $k_S = 2, 4$, so $K_P = 1$ and $K_S = 2$. Further, suppose both configurations are treated as basis registered with \mathcal{P} normal to the first coordinate axis, i.e. \mathcal{P} is the y -axis.

The configurations X_1 and X_2 are shown in the left and right figures in the top row of Figure 2 respectively, whereas the bottom row of Figure 2 show their corresponding reflections, where the left is for X_1 and $X_1^{(\text{refl})}$ and right is for X_2 and $X_2^{(\text{refl})}$. Note that X_1 is bilaterally symmetric, with $\mathbf{a} = \mathbf{0}$. Table 1 gives the $J_{\text{basis}} = 4$ elements of the vector \mathbf{a} for X_2 . The two elements for the landmark pair are listed first, and the two elements for the solos listed last, with

$$\mathbf{a} = (0.04, 0.18, 0.28, 0.31)^T$$

for X_2 . It can be seen visually in Figure 2 that for X_2 , landmarks 2 and 4 deviate more from the y -axis than the landmark pair (1, 3) differs from symmetry. Hence the last two components of \mathbf{a} are larger than the first two components.

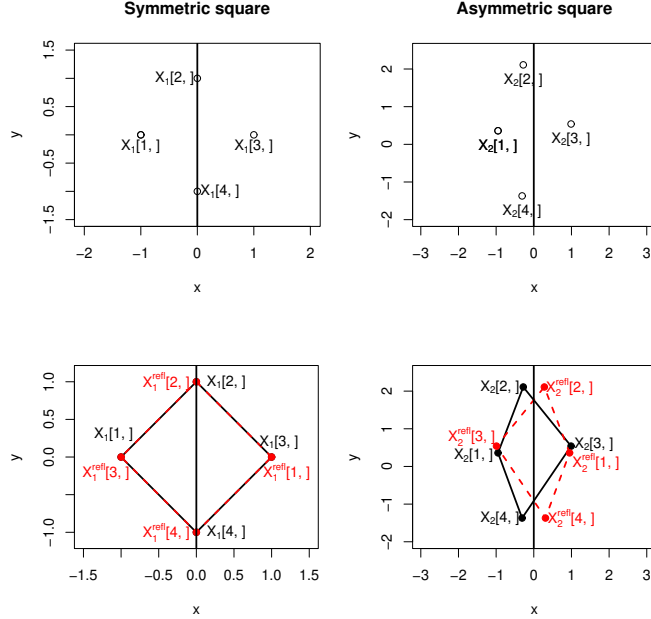


Figure 2: The left and right figures in the top row show the original configurations of symmetric square X_1 and asymmetric square X_2 (in black) respectively. The left and right figures in the bottom row show the original objects (in black solid lines) together with their respectively reflections $X_1^{(\text{refl})}$ and $X_2^{(\text{refl})}$ (in red dotted lines) respectively, in order to illustrate the coordinatewise elementary feature vector.

Table 1: Example in Section 2.3. Elements of the absolute elementary feature vector $\mathbf{a} \in \mathbb{R}^4$ for X_2 with $K = 4$ landmarks in $M = 2$ dimensions.

Landmark Indices	Coordinate Axis	Feature of \mathbf{a}	value of \mathbf{a}
Pair (1,3)	1	$a[(1, 3), 1] = X_2[1, 1] + X_2[3, 1] $	0.04
Pair (1,3)	2	$a[(1, 3), 2] = X_2[1, 2] - X_2[3, 2] $	0.18
Solo 2	1	$a[(2)] = X_2[2, 1] $	0.28
Solo 4	1	$a[(4)] = X_2[4, 1] $	0.31

3 Hypothesis tests

Consider a dataset of N basis registered configurations observed on two groups of individuals, where the first N_1 configurations belong to one group (Group 1) and the last N_2 configurations belong to the other group (Group 2), $N = N_1 + N_2$, where it is thought that the first group of configurations might be more symmetric than the second. One way to think about this question

is to construct a one-sided hypothesis test of

$$\begin{aligned} H_0 &: \text{the two groups have the same distribution of asymmetry vs.} \\ H_1 &: \text{Group 1 is more symmetric than Group 2.} \end{aligned} \tag{3.1}$$

For the paired data, we change the Group 1 and Group 2 in the above hypotheses to experimental and control groups respectively, where same subjects are contained in the two paired groups.

We will give two general approaches to construct a test statistic in order to compare the symmetries between the two groups: (a) combine-then-compare, where univariate test methods are used, and (b) compare-then-combine, where we form the hypotheses under union intersection test framework. These two approaches will be explored in the next subsections.

Suppose the data take the form of N registered configurations

$$X_n, n = 1, \dots, N. \tag{3.2}$$

Let \mathbf{a}_n denote the corresponding absolute elementary feature vector for X_n (equation (2.5)), with elements a_{nj} , $j = 1, \dots, J$ and $J = J_{\text{basis}}$ for the rest of this paper.

Then the hypotheses given in equation (3.1) can be reformulated as:

$$\begin{aligned} H_0 &: \mathbf{a}_n \sim F \text{ i.i.d. for all } n \text{ vs.} \\ H_1 &: \mathbf{a}_n \sim F_1 \text{ i.i.d. for } n = 1, \dots, N_1, \mathbf{a}_n \sim F_2 \text{ i.i.d. for } n = N_1 + 1, \dots, N, \end{aligned} \tag{3.3}$$

where F , F_1 , F_2 are multivariate cumulative density functions (c.d.f.s) and F_1 is stochastically smaller than F_2 (that is, $F_1(\mathbf{a}) \geq F_2(\mathbf{a})$ for all \mathbf{a} with at least one strict inequality, see, for example Stoyan (1983)). In other words, the distribution of F_2 is shifted towards right comparing with F_1 , which indicates more asymmetries. Under the paired data setting, \mathbf{a}_n for $n = 1, \dots, N_1$ represent the experimental data and \mathbf{a}_n for $n = N_1 + 1, \dots, N$ represent the control data, where $N = 2N_1$.

We concentrate in this section on t-test and Mann-Whitney U test. In Section 5, we further discuss some alternative univariate tests as well as multivariate tests in relation to the application

of Smile Data 1.

3.1 Testing strategy: combine-then-compare

Each element a_j of \mathbf{a} (equation (2.5)) is nonnegative and a larger value of a_j indicates greater asymmetry. Hence it is natural to reduce the J -dimensional vector \mathbf{a} to a single number by combining the elements of \mathbf{a} into a *composite asymmetry score*

$$u = \phi(\mathbf{a}), \quad (3.4)$$

say. Here the function $\phi(\mathbf{a})$ is assumed to be monotonically increasing in each component a_j when the other elements are held fixed.

Let $\psi(a)$ be a monotonically nonnegative increasing function of a scalar argument $a \geq 0$. Then one way to define $\phi(\mathbf{a})$ is as an *additive composite asymmetry score*

$$\phi_{\psi, \mathbf{w}}(\mathbf{a}) = \sum_{j=1}^J w_j \psi(a_j), \quad (3.5)$$

where the $w_j \geq 0$ are pre-assigned weights. Some choices for weights include the following:

- (a) equal weights $w_j = 1$,
- (b) greater weights near the midplane or away from the midplane, or
- (c) different weights for pairs and solos.

For example, in case (b), a weight might depend on $|X[k_R, 1] - X[k_L, 1]|$ for a landmark pair, with solos treated separately. The choices of weights in general depend on prior belief of the extent of asymmetry information carried by each landmark, for example, if it is known a priori that landmarks near \mathcal{P} can carry more important asymmetry information than landmarks far away from \mathcal{P} , then greater weights should be assigned to the nearer landmarks. For Smile Data 1, this information is available so greater weights will be given near the midplane, see Section 5.

Another way to give some elementary features greater prominence than others is through the choice of the functions ψ . For example, the quadratic function $\psi(a) = a^2$ is more sensitive to outlying features than the linear function $\psi(a) = a$.

We write below explicitly two such scores with equal weights and give them names L_1 and L_2 statistics respectively.

$$L_1 \text{ statistic: } \phi_{L_1}(\mathbf{a}) = \sum_{j=1}^J a_j = \sum_{(k_L, k_R)} \sum_{m=1}^M |d[(k_L, k_R), m]| + \sum_{k_S} |d[(k_S)]|, \quad (3.6)$$

$$L_2 \text{ statistic: } \phi_{L_2}(\mathbf{a}) = \sum_{j=1}^J a_j^2 = \sum_{(k_L, k_R)} \sum_{m=1}^M d[(k_L, k_R), m]^2 + \sum_{k_S} d[(k_S)]^2, \quad (3.7)$$

where the d 's are given in (2.1)-(2.3) and \mathbf{a} , a_j are given in (2.5).

We note that Bock and Bowman (2006) have proposed an asymmetry score which is proportional to ϕ_{L_2} , that is

$$\frac{2}{K} \phi_{L_2}(\mathbf{a}). \quad (3.8)$$

Further, Patel et al. (2023) uses the score given by

$$\phi_{L_1}^*(\mathbf{a}) = \sum_{(k_L, k_R)} d^*[(k_L, k_R)] + \sum_{k_S} d^*[(k_S)], \quad (3.9)$$

The $d^*[(k_L, k_R)]$ and $d^*[(k_S)]$ are defined in equation (2.4). Also, by squaring each element in the two sums in (3.9) and using (2.4), we recover ϕ_{L_2} :

$$\phi_{L_2}^*(\mathbf{a}) = \sum_{(k_L, k_R)} d^*[(k_L, k_R)]^2 + \sum_{k_S} |d^*[(k_S)]|^2 = \phi_{L_2}(\mathbf{a}). \quad (3.10)$$

Note that we can generalize $\phi^*(\mathbf{a})$ in the same way as $\phi(\mathbf{a})$ with weights. Instead of considering asymmetries with respect to each landmark as in (3.9), (3.6) and (3.7) view all features in \mathbf{a} as a whole and take the L_1 and L_2 norms. For the subjects which are more symmetric, their corresponding \mathbf{a}_n should be close to the origin. Hence, the L_1 and L_2 distances between \mathbf{a}_n with $\mathbf{0} \in \mathbb{R}^J$ are expected to be smaller for control subjects.

Table 2: The two composite asymmetry scores defined in equation (3.5) and equation (3.9) are computed on the configuration X_2 .

	$d^*[(1, 3)]$ (2.4)	$\phi_{L_1}(\mathbf{a})$ (3.6)	$\phi_{L_1}^*(\mathbf{a})$ (3.9)	$\phi_{L_2}(\mathbf{a})$ (3.7)
X_2	0.18	0.81	0.39	0.21

Example 1 continued. Recall the asymmetric square X_2 defined in equation (2.6). The configuration is shown in Figure 2. The landmark elementary feature, $d^*[(1, 3)]$, defined in equation (2.4) is computed and reported in Table 2. The composite asymmetry scores $\phi_{L_1}(\mathbf{a})$ (3.6), scaled $\phi_{L_1}^*(\mathbf{a})$ (3.9) (divided by the number of landmarks) and $\phi_{L_2}(\mathbf{a})$ (3.7) are computed on X_2 for illustration. The results are shown in Table 2. Note that the values of

$$d^*[(1, 3)] = \sqrt{(X_2[1, 1] + X_2[3, 1])^2 + (X_2[1, 2] - X_2[3, 2])^2} = 0.18$$

and $a[(2)] = 0.28$, $a[(4)] = 0.31$ (Table 1) are less than 1, so taking squares of them in ϕ_{L_2} leads to smaller values. Note that here we have scaled $\phi_{L_1}^*$ by a factor of half, so unscaled $\phi_{L_1}^* = 0.78$ which is similar to the value of $\phi_{L_1} = 0.81$.

Once a composite asymmetry score $\phi(\mathbf{a})$ has been chosen, let

$$u_n = \phi(\mathbf{a}_n), \quad n = 1, \dots, N, \quad (3.11)$$

denote the composite asymmetry scores for the data in (3.2).

Suppose u_n for $n = 1, \dots, N_1$ and $n = N_1 + 1, \dots, N$ are realizations from random variables U_1 and U_2 respectively, and let $g = 1, 2$ denote the control and cleft groups. Let

$$\mu_g = E\{U_g\}, \quad \sigma_g^2 = \text{var}\{U_g\} \quad (3.12)$$

denote the expectation and variance for a random variable $U_g \sim F_g$ (should not be confused with the distribution of the vector \mathbf{a} in Section 3). A simpler version of hypotheses in (3.1) is

$$H_0 : \mu_1 = \mu_2 \text{ vs. } H_1 : \mu_1 < \mu_2 \quad (3.13)$$

There are several test statistics that can be used for testing hypotheses given in (3.1) and (3.13), including the following:

- (a) Parametric test: the standard two-sample t-test, which assumes $\sigma_1^2 = \sigma_2^2$;
- (b) Non-parametric test: the Mann-Whitney U test, also known as the Wilcoxon rank sum test (Mann and Whitney, 1947).

In case (a), the significance of the test statistic under H_0 can be computed either analytically (assuming normality) or using a bootstrap approximation. In case (b) the significance can be derived from combinatorial arguments. Mann-Whitney U test is considered where the normality assumption on composite asymmetry scores $u_n = \phi(\mathbf{a}_n)$ may fail to hold.

Paired data The test strategies described above can be applied to the paired data by making necessary modification, namely we need to use the paired test in place of the two-sample test for both the parametric and non-parametric cases. Specifically, paired t-test and Wilcoxon signed-rank test are used for the parametric and non-parametric cases respectively.

An advantage of the combine-then-compare approach is that it enables us to accumulate evidence from different features, so if there is a small amount of asymmetry on many different elementary features, then the composite score will have a large value. Further, this approach enables the two groups to be compared visually with stem and leaf plots and in particular, any overlap between the two groups can be easily assessed. Applications of this approach are in Section 5.2.1, 6.2.1 and 6.3.1.

3.2 Testing strategy: compare-then-combine

In this approach, separate test statistics are constructed for each feature in the elementary feature vectors. The most extreme of these separate test statistics is then used as an overall test statistic. Before we give the details, the hypotheses in equation (3.1) need to be formulated in the Union

Intersection Test (UIT) style:

$$H_0 = \bigcap_{j=1}^J H_0^j \text{ vs } H_1 = \bigcup_{j=1}^J H_1^j, \quad (3.14)$$

where H_0^j : the mean of j th unsigned elementary feature between the two groups is the same, whereas H_1^j is that the mean of group 2 is larger than mean of group 1, for $j = 1, \dots, J$.

For each choice j of an unsigned elementary feature, we construct a statistic to compare the two groups, for example, a two-sample t-statistic or a Mann-Whitney U statistic. Denote the resulting statistics by v_j , $j = 1, \dots, J$. For example, if a t-statistic is used, then

$$v_j = (\bar{a}_j^{(1)} - \bar{a}_j^{(2)})/s_j. \quad (3.15)$$

where $\bar{a}_j^{(g)}$, $g = 1, 2$ are the sample means of the j th unsigned elementary feature in the two groups and s_j^2 is the corresponding pooled within-group variance.

Following Boyett and Shuster (1977), an overall UIT statistic to test H_0 vs H_1 in equation (3.14) can be defined by taking the maximum of these separate statistics,

$$V = \max_{j=1, \dots, J} v_j, \quad (3.16)$$

and Boyett and Shuster (1977) compute the critical points of V under the null hypothesis using bootstrap. The landmarks are correlated with each other, so the d_j are not independent for $j = 1, \dots, J$ here, so we cannot derive the distribution of V theoretically. Hence, the bootstrap has been used for estimating the critical points of V .

If there exists v_j which exceeds the critical value of V at a pre-determined significance level, then we not only know that the corresponding H_0^j is rejected (hence the overall H_0 in (3.14) is also rejected), but also know that the landmark corresponding to such v_j is important.

Our main aim is somewhat different from Boyett and Shuster (1977): we aim at discovering important landmarks while Boyett and Shuster (1977) focuses on estimating a p -value. Also, the

two bootstrap procedures are slightly different. Their procedure is as follows:

- (a) Construct a set E_n containing all random samples of size n taken without replacement from origin dataset $\{\mathbf{a}_i\}_{i=1}^N$.
- (b) Sample with replacement B times from this set E_n to form the bootstrap resampled dataset.
- (c) Compute the test statistic $\{V^{(1)}, \dots, V^{(B)}\}$ on the resampled dataset.
- (d) Compare the test statistic V computed on first n observed data $\{\mathbf{a}_i\}_{i=1}^n$ to $\{V^{(1)}, \dots, V^{(B)}\}$.

The procedure given in Boyett and Shuster (1977) does not perform bootstrap directly on the data, and only part of the data is used in either E_n or the observed statistic, which is probably to reduce the computational budget. In contrast, since our data size is not large and the computational budget is far more than enough, we directly sample with replacement from the whole dataset with $n = N$ and use all data to compute the observed statistic. Using all data is very likely to improve the final result. Our procedure is as follows:

- (a) Sample N samples with replacement from $\{\mathbf{a}_i\}_{i=1}^N$ and repeat this step B times.
- (b) Compute $\{V^{(1)}, \dots, V^{(B)}\}$ on resampled dataset.
- (c) Compare the test statistic V computed on all observed data $\{\mathbf{a}_i\}_{i=1}^N$ to $\{V^{(1)}, \dots, V^{(B)}\}$.

For compare-then-combine approach, we use a similar selection procedure to Tukey's method (Tukey, 1949) in ANOVA though in ANOVA a separate test statistic is used for each pairwise difference between main effects. Here, a separate test statistic for each j is more appropriate since the different features in the unsigned elementary feature vector \mathbf{a} measure different features of the face. An illustration is given below in Section 5.2.2 and 6.3.2.

Paired data The approach given in this section can be extended to the paired data scenario with the following changes applied to the bootstrap procedure.

- (a) Compute $a_{nj}^{(2)} - a_{nj}^{(1)}$ for each subject n and each feature j , where $a_{nj}^{(1)}$ and $a_{nj}^{(2)}$ are the feature j of vectors $\mathbf{a}_n^{(1)}$ and $\mathbf{a}_n^{(2)}$ for subject n from Group 1 and 2 respectively.

- (b) Assign +1 or -1 to each $\mathbf{a}_n^{(2)} - \mathbf{a}_n^{(1)}$ randomly with equal probability, which forms the permuted sample. Repeat this step B times.
- (c) Compute t -values on the permuted sample and record the largest t -value.

An illustration of this compare-then-combine approach is given below for the Smile Data 2 in Section 6.2.2.

4 Meta-Analysis Methods

We can consider the meta-analysis, which carries out simultaneous inference and also belongs to the compare-then-combine approach category. In particular in meta-analysis, we can obtain an overall p -value by combining the p -values from separate tests. We now give an overview for meta-analysis.

Suppose we have N basis registered configurations, where the first N_1 configurations are from Group 1 and the rest N_2 configurations are from Group 2. Absolute elementary feature vectors $\mathbf{a}_1, \dots, \mathbf{a}_N \in \mathbb{R}^J$ defined in equation (2.5) can be constructed on each configuration. Let $\mathbf{a}^{(g)}$ be the random vector associated to the population of group g and let $a_j^{(g)}$ denote feature j of vector $\mathbf{a}^{(g)}$, where $g = 1, 2$ for Group 1 and Group 2 respectively and $j = 1, \dots, J$.

Consider the J individual tests with corresponding hypotheses

$$H_0^j : a_j^{(1)} = a_j^{(2)}, \quad H_{1,L}^j : a_j^{(1)} < a_j^{(2)}, \quad H_{1,R}^j : a_j^{(1)} > a_j^{(2)}, \quad H_1^j : a_j^{(1)} \neq a_j^{(2)},$$

for $j = 1, \dots, J$. The p -values \tilde{p}_j and $1 - \tilde{p}_j$ correspond to the left and right alternative hypotheses $H_{1,L}^j$ and $H_{1,R}^j$ respectively. The two-sided p -value $p_j = 2 \min(\tilde{p}_j, 1 - \tilde{p}_j)$ corresponds to the two-sided alternative hypothesis H_1^j . The way of computing \tilde{p}_j and p_j depends on the choice of the univariate test.

One of such methodology to combine individual p -values is the well-known Fisher's method

(Fisher, 1932). The Fisher's combination function is given as:

$$P_L = -2 \sum_{j=1}^J \log(\tilde{p}_j), \quad P_R = -2 \sum_{j=1}^J \log(1 - \tilde{p}_j), \quad P = -2 \sum_{j=1}^J \log(p_j), \quad (4.1)$$

which correspond to the left, right and two-sided overall alternative hypotheses. P_L , P_R and P all follow $\chi_{2,J}^2$ -distribution. Hence, a final p -value is obtained by comparing them with the tail of the $\chi_{2,J}^2$ -distribution.

For the Fisher's method, P_L is used in our illustrative smile examples but not P or P_R , since we would like to test whether the values of absolute elementary features from Group 1 are smaller than the feature values from Group 2. In other words, we are interested in the left-sided tests. However, the right-sided and two-sided tests could be relevant for some other practical examples.

There is another combination function based on Pearson (1934) which is given as

$$Q = \max(P_L, P_R), \quad (4.2)$$

which does not follow a χ^2 -distribution. Hence, randomization tests and permutation tests are used to estimate the overall p -value in two-sample and paired data cases respectively. For the randomization tests, the procedures are given as below:

- (a) Sample without replacement from the pooled dataset of the two groups for B times.
- (b) Perform individual two-sample tests on the resampled data and obtain p -values $\tilde{p}_j^{(b)}$ and $1 - \tilde{p}_j^{(b)}$, for $j = 1, \dots, J$ and $b = 1, \dots, B$.
- (c) Compute the overall p -values defined in equation (4.1) and hence Q defined in (4.2).

The procedures for permutation tests are given as the following:

- (a) Shuffle the subjects randomly, such as change the subjects between experimental group to control group while keeping the paired structure. Repeat this step for B times.
- (b) Perform individual paired tests to obtain p -values $\tilde{p}_j^{(b)}$ and $1 - \tilde{p}_j^{(b)}$, for $j = 1, \dots, J$ and

$$b = 1, \dots, B.$$

(c) Compute the overall p -value defined in equation (4.1) and hence Q defined in (4.2).

We use $B = 10000$ in both randomization and permutation tests.

The choice between Fisher’s method and Pearson’s method depend on the problem at hand and Owen (2009) provides a review of both methods. In particular, if we suspect there are large deviations from individual null hypotheses, then Pearson’s method has higher power than Fisher’s method; the paper also shows that the Pearson’s method is admissible.

The difference between the feature selection (see Section 3.2) and the Fisher’s and Pearson’s methods is that in the first approach, we record the test statistics resulted in each single test and use an overall test statistics to combine them together. Hence, obtaining a final p -value or carrying out feature selection are both possible. In the second approach, we combine the p -values obtained from each individual test together via a pre-defined combination function and calculate a final p -value. We cannot proceed the feature selection by using this method. The applications of the Fisher’s and Pearson’s methods on the two illustrative smile examples are given in Section 5.2.2, 6.2.2 and 6.3.2 respectively.

5 Analyses of the Cleft Lip Smile Data

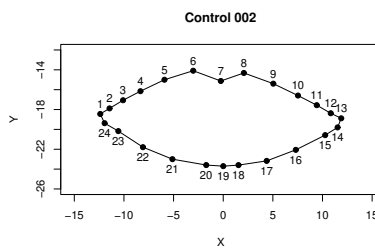
5.1 Details

We now illustrate the methods using the cleft lip smile data. The data is collected using the Di4D system (Patel et al., 2023) as described in Section 2 and it has been pre-registered using the basis registration. This data contains $N = 25$ subjects, of which $N_1 = 12$ are control subjects and $N_2 = 13$ are cleft subjects. There are $K = 24$ landmarks on the lip periphery. Figure 3 shows the lip configuration in the x - y plane. There are $K_P = 11$ landmark pairs and $K_S = 2$ solo landmarks. The landmark indices are summarized in Table 3. The $M = 3$ dimensional coordinates of these landmarks have been extracted at three frames: first (closed lip), middle (middle of the smile)

Table 3: Indices of landmark pairs and solos in Figure 3 on the lip periphery for the Smile Data 1.

Landmark notation	Indices in Figure 3
pair (k_L, k_R)	$(1,13), (2,12), (3, 11), (4,10), (5,9), (6,8), (20,18), (21,17), (22,16), (23,15), (24,14)$
k_S	7, 19

and last frame (maximum open lip smile). We have $J = MK_P + K_S = 35$. Let $g = 1, 2$ denote the control and cleft groups, respectively.

Figure 3: Landmark indices for x - y coordinates on the lip periphery of a control subject at first frame from Smile Data 1.

In the rest of this section several test statistics as described in Section 3 will be presented under two headings “combine-then-compare approach” and “compare-then-combine approach”.

5.2 Test Results for Smile Data 1

5.2.1 Application of the Combine-then-compare Approach

Patel et al. (2023) carried out standard two-sided two-sample t-tests using the statistic (3.9), with conventional t-tables used to judge significance. Here we report the results of the one-sided versions of these t-tests since based on hypotheses in (3.1), one-sided tests are more appropriate. The results of our t-tests are given in Table 4. We reach the same conclusions as in Patel et al. (2023) for their two-sided tests, namely, H_0 is rejected at all three frames. Further, the one-sided t-test indicates that there is more asymmetry for cleft lip subjects versus controls. Note that here the p -value is the smallest at the first frame, which suggests that the two groups are the most different at the beginning of the smile.

Then, we use the scores $\phi_{L_1}(\mathbf{a})$ and $\phi_{L_2}(\mathbf{a})$ defined in equations (3.6) and (3.7) respectively.

Table 4: Mean, variance, t-values and p -values for $\phi_{L_1}^*(\mathbf{a})$ using Smile Data 1 (equation (3.9)) for cleft and control subjects at first, middle and last frames (Patel et al. (2023)).

	Cleft		Control		t -values	One-sided test	Two-sided test
	mean	sd	mean	sd		p -values	p -values
First	21.35	5.54	13.39	5.11	-3.72	0.0006(***)	0.0011(**)
Middle	23.57	8.37	17.35	5.87	-2.13	0.02(*)	0.04(*)
Last	25.65	9.66	18.22	5.21	-2.36	0.01(*)	0.03(*)

(*) = significant at the 5% significance level. (**) = significant at the 1% significance level. (***) = significant at the 0.1% significance level.

Table 5: p -values from one-sided two-sample Mann-Whitney U tests using $\phi_{L_1}(\mathbf{a})$ (3.6) and $\phi_{L_2}(\mathbf{a})$ (3.7) based on Smile Data 1.

Composite asymmetry score	First frame	Middle frame	Last frame
$\phi_{L_1}(\mathbf{a})$	0.0001(***)	0.043(*)	0.011(*)
$\phi_{L_2}(\mathbf{a})$	0.0008(***)	0.026(*)	0.020(*)
weighted $\phi_{L_1}(\mathbf{a})$	0.0008(**)	0.004(**)	0.002(**)
weighted $\phi_{L_2}(\mathbf{a})$	0.002(*)	0.015(*)	0.006(**)

(*) = significant at the 5% significance level. (**) = significant at the 1% significance level. (***) = significant at the 0.1% significance level.

Several one-sided two-sample Mann-Whitney U tests have been performed and the results are shown in Table 5. For the last two rows in the table, the weighted $\phi_{L_1}(\mathbf{a})$ and weighted $\phi_{L_2}(\mathbf{a})$ are used and w_j are chosen in an adaptive way as the following:

- (a) Compute the sample mean shape on the doubled dataset, which contains basis registered original configurations and their reflections through midplane. Since the data has been pre-registered, the sample mean shape is simply the arithmetic mean for each landmark.
- (b) The Euclidean distance within each landmark pair for this mean shape is computed and its reciprocal is used as the weight. The weights are the same for all 25 subjects. The weights for solo landmarks are the unit length based on the scale of data ($w_j = 1$ in (3.6) and (3.7)).

Different landmarks carry different amount of asymmetry information. Those landmarks near the midplane \mathcal{P} may carry the most significant information on asymmetry according to the expert's knowledge. Thus, we give higher weights to landmarks near \mathcal{P} and smaller weights on landmarks faraway from the central.

It can be seen from Table 5 that H_0 is rejected in all cases. In summary, there are significant differences between cleft and control subjects at all frames, with control subjects less asymmetric

than cleft subjects overall.

5.2.2 Application of the Compare-then-combine Approach

Feature selection The method described in Section 3.2 is used to select the landmarks which possess significant asymmetry information. v_j is selected to be the two-sample t-statistics (equation (3.15)). V defined in (3.16) is computed and its critical value at 5% significance level is determined via bootstrap. The total number of bootstrap iterations used was 10000. Boyett and Shuster (1977) has suggested 17000 iterations to make sure the significance level is 1%. However, the results of using 10000 and 17000 iterations turned out to be the same for our Smile Data 1. The central pair, landmarks 6 and 8, corresponds to t -values which exceed these critical points at all three frames. Thus, these two landmarks carry the most significant information of asymmetry.

Further, most of the extreme p -values obtained from Mann-Whitney U tests are related to landmarks 6, 8 and two solo landmarks 7 and 19. These tests are performed using ϕ_{L_1} and ϕ_{L_2} computed on various subsets of landmarks. This suggests that the two groups are differed at most when using these four landmarks. So these landmarks can carry important information on asymmetries. This finding matches the expert's opinion. Figure 4 shows a photo of a cleft patient, where the central pair (6, 8) and solo landmarks, 7 and 19, are marked on the photo and the landmarks are same as in Figure 3. Roughly, it is a 'Y'-shape if we join the landmarks 6, 7, 8 and then 7 with 19 by line segments. From medical point of view, this particular shape is known a priori to be the most important for the asymmetry assessment.

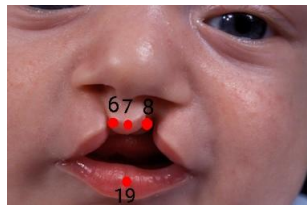


Figure 4: Photo of a cleft patient with central pair landmarks and solo landmarks. This figure is reproduced from photo taken from the website <https://www.nhs.uk/conditions/cleft-lip-and-palate/>.

Meta-analysis Fisher's method and Pearson's method defined in equation (4.1) and (4.2)

Table 6: The results of P_R and p -values obtained from Fisher’s method and Pearson’s method at all three frames using the Smile Data 1.

	P_L	P_R	Q	Fisher’s method	Pearson’s method
First frame	206.65	12.26	206.65	0(***)	4×10^{-4} (***)
Middle frame	127.19	33.90	127.19	3.51×10^{-5} (***)	0.067
Last frame	134.21	26.89	134.21	6.18×10^{-6} (***)	0.027(*)

(*) = significant at the 5% significance level. (**) = significant at the 1% significance level. (***) = significant at the 0.1% significance level.

respectively are performed. Mann-Whitney U test is used to obtain individual left-sided p -values, \tilde{p}_j , for $j = 1, \dots, 35$, using \mathbf{a}_n , $n = 1, \dots, 25$.

For Fisher’s method, we compare P_L with the tail of χ_{70}^2 distribution (as $J = 35$) to obtain overall p -values. For the Pearson’s method, randomization tests with 10000 iterations are used to estimate the overall p -values. The values of P_L , P_R , Q and p -values derived at the three frames are shown in Table 6. H_0 is rejected at all frames when we use Fisher’s method. For Pearson’s method, H_0 is rejected at the first and last frames. Comparing with Table 4 and 5, the p -values for the Fisher’s method are more extreme. This indicates that Fisher’s method is more sensitive to the departures of cleft group from control group.

5.2.3 Welch’s t -test and Hotelling’s T^2 Test

There are a few other tests we have applied and could be relevant for some future applications

- (a) The Welch version of the t -test (Welch (1947), Lehmann and Romano (2005)), which accommodates different variances for the two groups. In this example, the results of the Welch t -test is found to be similar to the standard t -test (Table 4). A possible reason is that our sample size is small, so it results in similar outcomes.
- (b) Hotelling’s T^2 test (Mardia et al., 2024). We apply here Hotelling’s T^2 test on unsigned elementary feature vector \mathbf{a}_n , $n = 1, \dots, N$. In this example, we reject H_0 for the first two frames at 5% significance level. The reason could be that a Hotelling’s T^2 test treats the features separately so it does not gain any power if the features point in the same direction; one-sided Hotelling’s T^2 could be an appropriate approach, which we will pursue in future.

In this example of Smile Data 1, the sample size is less than the dimension of \mathbf{a}_n , i.e. $N < J$, so the covariance matrix is singular, which requires some modifications and will be dealt in future.

5.3 Visual Study Related to Three Composite Statistics

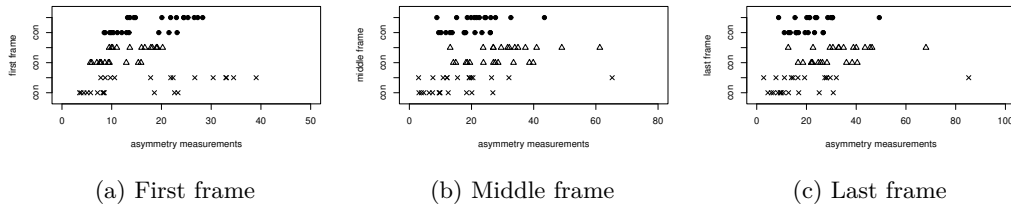


Figure 5: Plots for three composite asymmetry scores. From top to bottom, we have $\phi_{L_1}^*(\mathbf{a})$ (3.9) (in solid dots), $\phi_{L_1}(\mathbf{a})$ (3.6) (in triangles) and $\phi_{L_2}(\mathbf{a})$ (3.7) (in crosses) at the three frames computed on the Smile Data 1. Plot (a) is at first frame, while (b) is at middle frame, whereas (c) is at last frame. In plot (a), $\phi_{L_1}(\mathbf{a})$ and $\phi_{L_2}(\mathbf{a})$ are divided by 2. In plot (b) and (c), $\phi_{L_2}(\mathbf{a})$ is divided by 3. The first, third and fifth rows from top to bottom are left while others are control.

Since the test results indicate significant differences between the two groups, we would like to visualize the distributions of $\phi_{L_1}^*(\mathbf{a})$, $\phi_{L_1}(\mathbf{a})$ and $\phi_{L_2}(\mathbf{a})$ defined in (3.9), (3.6) and (3.7) respectively between the two groups. Hence, dot plots similar to the stem leaf plot are created and given in Figure 5. In these dot plots, composite asymmetry scores for both groups are plotted together at each frame. According to these dot plots, substantial overlaps between cleft and control subjects can be seen. Moreover, the three scores used in this section all have similar performances, as the separation between the two groups at each frame revealed by the dot plots are all similar.

Figure 6 shows the dot plots for weighted $\phi_{L_1}(\mathbf{a})$ and weighted $\phi_{L_2}(\mathbf{a})$ simultaneously. According to these figures, these two composite scores push outliers farther away from the rest of the samples, more so for weighted ϕ_{L_1} .

5.4 Summary of the Analyses

We end this section by summarizing the main conclusions for these cleft lip data:

- (a) There are statistically significant differences between the two groups at all frames. The

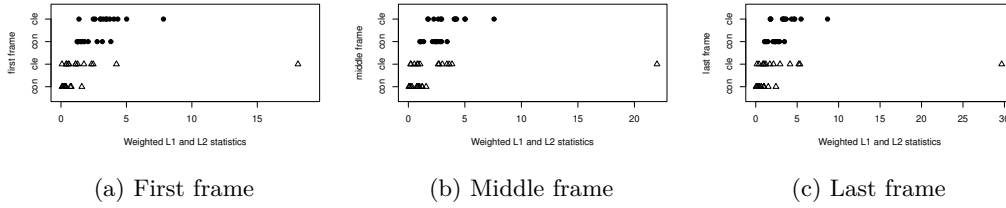


Figure 6: Plots of two weighted asymmetry scores. From top to bottom, we have weighted $\phi_{L_1}(\mathbf{a})$ (in solid dots) and $\phi_{L_2}(\mathbf{a})$ (in triangles) at the three frames computed using the Smile Data 1. The first and third rows from top to bottom are left while others are control. Plot (a) is at first frame, while (b) is at middle frame, whereas (c) is at last frame.

control subjects are overall more symmetric than the cleft lip subjects.

(b) Substantial overlaps can be found on dot plots in Figure 5. This matches the expert's expectation that some cleft lip subjects should be fairly close to normal subjects after surgeries.

(c) The landmarks 6, 7, 8 and 19 (the 'Y'-shape) are the most important in assessing asymmetries.

6 Analyses of the Orthognathic Surgery Smile Data

6.1 Details

The orthognathic surgery smile data contains $N = 22$ subjects who have undergone orthognathic surgery and their pre- and post-surgery data have both been collected. Figure 7 shows the face before (in the left) and after (in the right) the orthognathic surgery, where the view is from the right side of the face. It can be seen in the left of Figure 7, the jaw is somewhat protruded in comparison to the figure on right.

The axes used for the Smile Data 2 are exactly the same as the Smile Data 1 and the details are given in Section 2.1. The 16 landmarks on the nasal region are shown in left of Figure 8, while the right of Figure 8 shows the 10 landmarks on the lip. The landmark indices are summarized in Table 7. The scale of the Smile Data 2 is in mm. The same frames as the Smile Data 1 are used.

There are two sets of landmarks we will focus on:



Figure 7: View of the face from right before (left) and after (right) the orthognathic surgery.

Table 7: Indices of landmark pairs and solos in Figure 8 on the lip periphery and nasolabial region for the Smile Data 2.

Landmark notation	Indices in Figure 8
pair (k_L, k_R)	$(1,7), (2,6), (3, 5), (8,10), (11,12), (15,16)$
k_S	4, 9, 13, 14

- (a) The 7 landmarks on the upper lip (landmarks 1 to 7 in Figure 8) and the 6 landmarks on the nasal region (landmarks 11 to 16 in the left of Figure 8). There are $K_P = 5$ paired landmarks and $K_S = 3$ solo landmarks, hence, $J = 18$.
- (b) The 10 landmarks on the lip (landmarks 1 to 10 in Figure 8). There are $K_P = 4$ paired landmarks and $K_S = 2$ solo landmarks, hence, $J = 14$.

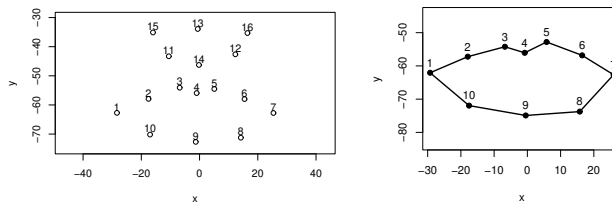


Figure 8: The left figure shows the 16 landmarks on the nasolabial region for a typical subject at the first frame using the pre-surgery data. The right figure shows the 10 landmarks on the lip periphery. The two figures are based on the Smile Data 2.

These two sets of landmarks correspond to two aims:

- (a) Assess the affects of surgery, by comparing pre- and post-surgery data via paired tests (item (a) above).

- (b) Compare the subjects from Smile Data 2 to the control subjects from the Smile Data 1 where we use the same landmarks on the lip for both data (item (b) above).

Some previous studies have been carried out, such as in Al-Hiyali et al. (2015), Xue et al. (2020), Xue et al. (2023) and Quast et al. (2023). These studies have focused on different facial expressions and the authors have taken average over measurements resulted from these expressions. However, by doing this, they would lose a lot of information. Our work is different from these previous studies as we attempt to construct asymmetry measurements over the lip and nasal region at different frames during the smile.

The rest of this section will be divided into two parts corresponding to item (a) (effect of surgery, see Section 6.2) and item (b) (deviation from normal subjects, see Section 6.3) above.

6.2 Test Results for Smile Data 2: Effect of Surgery

The pre-surgery data is compared to the post-surgery data by using one-sided paired tests on the asymmetry measurements. Let $g = 1, 2$ denote the pre-surgery data and post-surgery data respectively. The absolute elementary feature vectors $\mathbf{a}_n^{(1)}$ and $\mathbf{a}_n^{(2)}$ are computed using the pre- and post-surgery data separately, for $n = 1, \dots, 22$.

6.2.1 Application of the Combine-then-compare Approach

The 13 landmarks on the upper lip and nasal region are used. Paired t-tests have been performed on composite asymmetry scores defined in equation (3.9) whereas Wilcoxon signed-rank tests have been performed on scores defined in (3.6), (3.7) respectively.

Since the expert suspects that the asymmetries are increased after the surgery, so the one-sided alternative hypothesis becomes the distribution relates to pre-surgery data is stochastically smaller than that of post-surgery data. The Group 1 and Group 2 in (3.1) are changed to pre- and post-surgery data respectively.

The test results on $\phi_{L_1}^*$ given in equation (3.9) are shown in Table 8. H_0 is rejected in middle and last frames. In other words, the asymmetries are increased after surgery when inspect at these

Table 8: Mean, variance, t-values and p -values using $\phi_{L_1}^*(\mathbf{a})$ based on the Smile Data 2 (equation (3.9)).

$\phi_{L_1}^*(\mathbf{a})$	Pre		Post		t -values	One-sided paired test
	mean	sd	mean	sd		p -values
First	15.69	5.64	18.47	8.49	-1.33	0.098
Middle	17.53	5.92	22.25	10.89	-2.36	0.014(*)
Last	17.72	5.45	22.77	9.52	-3.29	0.002(**)

(*) = significant at the 5% significance level. (**) = significant at the 1% significance level. (***) = significant at the 0.1% significance level.

Table 9: p -values from one-sided Wilcoxon signed-rank tests using $\phi_{L_1}(\mathbf{a})$ (3.6) and $\phi_{L_2}(\mathbf{a})$ (3.7) based on the Smile Data 2.

Composite asymmetry score	First frame	Middle frame	Last frame
$\phi_{L_1}(\mathbf{a})$	0.13	0.016(*)	0.002(**)
$\phi_{L_2}(\mathbf{a})$	0.088	0.007(**)	0.001(**)

(*) = significant at the 5% significance level. (**) = significant at the 1% significance level. (***) = significant at the 0.1% significance level.

two frames. Further, the p -value is the most extreme at the last frame, which indicates that the two groups are the most different at the last frame.

Table 9 displays the results of Wilcoxon signed-rank tests on $\phi_{L_1}(\mathbf{a})$ given by (3.6) and $\phi_{L_2}(\mathbf{a})$ given by (3.7). We reach the same outcomes as the paired t-tests: H_0 is rejected at the middle and last frames and the two groups are the most different at the last frame.

6.2.2 Application of the Compare-then-combine Approach

Feature selection The procedures given in Section 3.2 are performed using pre- and post-surgery data, in order to select which landmarks contribute the most to the increment in asymmetries after the surgery. 10000 bootstrap iterations are performed. The 25%, 20%, 15% and 10% critical values of V are determined at the three frames separately. The corner pair, landmarks (1, 7) are important at the middle frame with respect to 25%, 20% and 15% critical values of V . The significance levels used here are larger than we used for Smile Data 1 in Section 5, which implies the features selected here are less important than the features in Smile Data 1.

Meta-analysis Fisher's method and Pearson's method given in (4.1) and (4.2) are performed with Wilcoxon signed-rank tests as individual tests using $\mathbf{a}_n^{(1)}$ and $\mathbf{a}_n^{(2)}$, for $n = 1, \dots, 22$. P_L

Table 10: The results of P_R and p -values obtained from Fisher’s method and Pearson’s method at all three frames. Pre- and post-surgery data from the Smile Data 2 is used here.

	P_L	P_R	Q	Fisher’s method	Pearson’s method
First frame	45.52	20.04	45.52	0.13	0.45
Middle frame	63.39	10.09	63.39	0.003(**)	0.085
Last frame	64.20	11.53	64.20	0.003(**)	0.041(*)

(*) = significant at the 5% significance level. (**) = significant at the 1% significance level. (***) = significant at the 0.1% significance level.

defined in equation (4.1) is computed and compare with the tail of χ_{36}^2 distribution (as $J = 18$).

As for Q , permutation tests are used to estimate the overall p -values. Table 10 shows the values of P_L , P_R , Q and p -values for Fisher’s and Pearson’s method at the three frames.

For the Fisher’s method, we obtain the same results as in the combine-then-compare approach: H_0 is rejected at middle and last frames. However, the p -values obtained in Fisher’s method are more extreme at the middle frame than those from combine-then-compare approach. For the Pearson’s method, we fail to reject H_0 at the first and middle frames. This indicates that the Pearson’s method may not be sensitive to changes in asymmetries before and after the surgery.

6.3 Test Results for Smile Data 1 and Smile Data 2: Deviation from Control Subjects

The Smile Data 2 is compared with the control subjects from the Smile Data 1. In Section 5, we only use 12 subjects which form a subset of the control group. The expert believes that more data should be used, thus, all 109 control subjects are used in this section. To make the comparisons available, a subset of 10 landmarks on the lip (Figure 8) are chosen from the 24 landmarks (see Figure 3), so that the Smile Data 2 and the Smile Data 1 have the same landmarks at the lip. Hence, the absolute elementary feature vectors \mathbf{a}_n for $n = 1, \dots, 12$ are recomputed on the subjects from Smile Data 1 using the new landmarks. Pre- and post-surgery data are used separately. Hence, we have three groups in total, but we stick with two-sample tests. We scale the data so that both datasets have the same scale in cm.

Table 11: p -values from one-sided two-sample Welch's t -test using $\phi_{L_1}^*$ defined in (3.9) to compare between Smile Data 2 subjects with normal subjects from the Smile Data 1.

$\phi_{L_1}^*$	First frame	Middle frame	Last frame
Pre-surgery	0.006(**)	0.073	0.031(*)
Post-surgery	0.025(*)	0.013(*)	0.010(*)

(*) = significant at the 5% significance level. (**) = significant at the 1% significance level. (***) = significant at the 0.1% significance level.

Table 12: Mean, standard deviation, t-values of $\phi_{L_1}^*(\mathbf{a})$ (equation (3.9)) for pre-, post-surgery subjects from Smile Data 2 and 12 control subjects from Smile Data 1.

$\phi_{L_1}^*(\mathbf{a})$	Pre		Post		Control	
	mean	sd	mean	sd	mean	sd
First	0.95	0.35	0.87	0.29	0.74	0.22
Middle	1.17	0.41	1.30	0.52	1.03	0.35
Last	1.22	0.34	1.32	0.46	1.07	0.33

Table 13: p -values obtained from one-sided two-sample Mann-Whitney U tests using ϕ_{L_1} in (equation (3.6)) and ϕ_{L_2} in (3.7) to compare between Smile Data 2 subjects with control subjects from the Smile Data 1.

	Pre		Post	
	ϕ_{L_1}	ϕ_{L_2}	ϕ_{L_1}	ϕ_{L_2}
First	0.0044(**)	0.0050(**)	0.059	0.070
Middle	0.062	0.060	0.0081(**)	0.014(*)
Last	0.018(*)	0.040(*)	0.0030(**)	0.0037(**)

(*) = significant at the 5% significance level. (**) = significant at the 1% significance level. (***) = significant at the 0.1% significance level.

6.3.1 Application of the Combine-then-compare Approach

The one-sided two-sample t -tests are performed on $\phi_{L_1}^*$ defined in (3.9) and the outcomes are shown in Table 11. Table 12 shows the means and variances of $\phi_{L_1}^*$ for the three groups of data. H_0 is rejected in almost all cases, except for the pre-surgery data at middle frame. This implies that in most of the cases, control subjects from the Smile Data 1 are more symmetric than subjects from the Smile Data 2 .

One-sided two-sample Mann-Whitney U tests have been performed using ϕ_{L_1} and ϕ_{L_2} defined in (3.6) and (3.7) respectively. The test results are shown in Table 13. H_0 is rejected in almost all cases except for pre-surgery data at the middle frame and post-surgery data at the first frame.

However, the test results violate the expert's observations: both pre- and post-surgery data

Table 14: p -values obtained from one-sided two-sample Mann-Whitney U tests using ϕ_{L_1} in (equation (3.6)) and ϕ_{L_2} in (3.7), where $w_j = 1$ for pairs and $w_j = 2$ for solos, to compare between Smile Data 2 subjects with control subjects from the Smile Data 1.

	Pre		Post	
	ϕ_{L_1}	ϕ_{L_2}	ϕ_{L_1}	ϕ_{L_2}
First	0.0047(**)	0.0035(**)	0.026(*)	0.018(*)
Middle	0.073	0.075	0.0055(**)	0.0073(**)
Last	0.015(*)	0.042(*)	0.0018(**)	0.0026(**)

(*) = significant at the 5% significance level. (**) = significant at the 1% significance level. (***) = significant at the 0.1% significance level.

are asymmetric at the first frame and the pre-surgery data is more asymmetric at this frame. We then compute the ϕ_{L_1} and ϕ_{L_2} with different weights for the solos, where the weights for the solos are the doubled unit lengths ($w_j = 2$ in (3.6) and (3.7)) while we still keep the weights for landmark pairs to be unit length ($w_j = 1$ in (3.6) and (3.7)). The test results from Mann-Whitney U tests are displayed in Table 14. H_0 is rejected for both groups at the first frame. Further, the p -values for pre-surgery group is more extreme, which indicates that the pre-surgery data are more asymmetric. This findings match the expert's opinion. Note that changing the weights in this way do not affect the results for compare-then-combine approach.

The patterns of the p -values shown in Table 11, 13 and 14 are the same: the pre-surgery data has smaller p -values at the first frame, whereas the post-surgery data has more extreme p -values at the middle and last frames.

6.3.2 Application of the Compare-then-combine Approach

Feature selection The method described in Section 3.2 is used to select the landmarks which possess significant asymmetry information for the pre- and post-surgery data when compare with the normal subjects. v_j is selected to be the two-sample t-statistics (equation (3.15)). V defined in (3.16) is computed and its critical value at 5% significance level is determined via bootstrap. The total number of bootstrap iterations used is 10000.

The central pair, landmarks (3, 5), possesses t-values which exceed the critical values of V in most of the cases for both pre- and post-surgery data. The solo landmark 9 also corresponds to t-values exceed the critical values of V in some cases. Most of the extreme p -values obtained from

Table 15: The results of P_R and p -values obtained from Fisher’s method and Pearson’s method at all three frames. Pre-surgery data from the Smile Data 2 is compared with the control subjects from the Smile Data 1 here.

	P_L	P_R	Q	Fisher’s method	Pearson’s method
First frame	9.54	67.13	67.13	$4.63 \times 10^{-5}(***)$	0.003(**)
Middle frame	22.25	46.44	46.44	0.016(*)	0.11
Last frame	17.16	51.90	51.90	0.0039(**)	0.038(*)

(*) = significant at the 5% significance level. (**) = significant at the 1% significance level. (***) = significant at the 0.1% significance level.

Mann-Whitney U tests pertain to the central pair 3, 5 and two solos, 4 and 9, where ϕ_{L_1} and ϕ_{L_2} are used. Landmark pair (3, 5) is the same as landmark pair (6, 8) and solo landmarks 4 and 9 are the same as landmarks 7 and 19 in Figure 4, so we recover the ‘Y’-shape as in Section 5.

Meta-analysis The Fisher’s and Pearson’s methods given in (4.1) and (4.2) are executed to compare the subjects from Smile Data 2 with control subjects from the Smile Data 1. P_R defined in equation (4.1) is computed at the three frames separately and compared with the tail of χ_{28}^2 (as $J = 14$).

Pre-surgery data Table 15 shows the results at the three frames which are obtained by comparing pre-surgery data with control subjects. Comparing with Table 11 and 14, H_0 is also rejected at the middle frame for the Fisher’s method and the p -values are more extreme at the first and last frames. The reason could be that the means of some asymmetry features are different for the two groups. However, these features have small magnitudes, so they do not contribute significantly towards the values of composite scores. Consequently, they do not affect the test results on the composite scores, but impact the outcomes of Fisher’s method. Nevertheless, for the Pearson’s method, the results are the same as in Table 11 and 14 and the magnitudes of p -values are similar as well.

Post-surgery data Table 16 shows the results obtained by comparing post-surgery data and control subjects. We obtain the same test results as in Table 11 and 14. The magnitudes of p -values for Pearson’s method are similar with the p -values obtained for ϕ_{L_1} and ϕ_{L_2} at the middle and last frames, whereas the p -value is decreased at the first frame for Pearson’s method. For Fisher’s method, the p -values are more extreme.

Table 16: The results of P_L and p -values obtained from Fisher’s method and Pearson’s method at all three frames. Post-surgery data from the Smile Data 2 is compared with the control subjects from the Smile Data 1 here.

	P_L	P_R	Q	Fisher’s method	Pearson’s method
First frame	14.26	67.61	67.61	$3.98 \times 10^{-5} (***)$	0.003 (**)
Middle frame	10.83	70.64	70.64	$1.51 \times 10^{-5} (***)$	0.004 (**)
Last frame	13.64	63.86	63.86	0.00013 (***)	0.009 (**)

(*) = significant at the 5% significance level. (**) = significant at the 1% significance level. (***) = significant at the 0.1% significance level.

6.4 Summary of the Analyses

We end the section by summarizing our findings on the orthognathic surgery data:

- (a) The asymmetries are increased after the surgery at middle and last frames.
- (b) The subjects contained in the Smile Data 2 are more asymmetric than the control subjects from the Smile Data 1, except for the pre-surgery data at the middle frame.
- (c) The central pair and solo landmarks, i.e. the ‘Y’-shape in Figure 4, carry important asymmetry information when we compare the subjects in Smile Data 2 with control subjects from Smile Data 1.

7 Discussion

We have presented our asymmetry measures for the registered Smile Data. But these asymmetry measures are available to any registered dataset. Further, we have used only a size-and-shape framework but the composite measures can be extended easily to include for example, similarity shape, since once we have registered the shapes, the asymmetry measures are applicable after allowing for scaling.

We have used absolute values (a_j) on coordinate elementary features as in equation (2.5) which is of main interest if one is looking for the extent of asymmetry as in our cases for the illustrative smile examples. However, there maybe some other applications where raw d_j may be important than a_j , such as when analyzing the trajectories of the landmarks; our work easily applies to that situation.

In this paper we have concentrated on the illustrative smile examples with three fixed frames and our future statistical work will be extended to dynamic shape analysis which will allow us to study trajectories of the smile.

In our case, the number of landmarks K is small but when K is large we can study the distribution of asymmetry measure ϕ_{L_2} under isotropic normality and various tests can be then performed. The work leads to understanding for the sum of weighted χ^2 -distributions. Mardia and Wu (2025) studies this approach.

We have used mostly univariate methods except for the Hotelling's T^2 in Section 5, though in our case, the sample size is less than the dimension of the elementary feature vector so it is not appropriate as Hotelling's T^2 is singular. Even in the case when the sample size is large enough, the one-sided alternative seems natural according to equation (3.1). Such cases are also part of our future investigation.

We note that the final aim of our work is to provide in future a smile index based on these asymmetry measures to be used as a standard index in clinics.

Data Availability Statement

The codes and data for this paper are available at the following website: <https://github.com/XW-2025-hub/JRSS-C-Supplementary-Materials>.

Acknowledgments

The authors would like to thank the School of Mathematics, and the School of Dentistry University of Leeds for supporting the smile project; we are also grateful to Fred Bookstein for collaborating with this project. The authors would also like to thank Sofya Titarenko for her helpful comments. Kanti Mardia acknowledges the Leverhulme Trust for the Emeritus Fellowship.

References

- Ajmera, D. H., Hsung, R. T., Singh, P., Wong, N. S. M., Yeung, A. W. K., Lam, W. Y. H., Khambay, B. S., Leung, Y. Y. and Gu, M. (2022) Three-dimensional assessment of facial asymmetry in class III subjects. Part 1: a retrospective study evaluating postsurgical outcomes. *Clinical Oral Investigations*, **26**, 4947–4966.
- Ajmera, D. H., Zhang, C., Ng, J. H. H., Hsung, R. T., Lam, W. Y. H., Wang, W., Leung, Y. Y., Khambay, B. S. and Gu, M. (2023) Three-dimensional assessment of facial asymmetry in class III subjects. Part 2: evaluating asymmetry index and asymmetry scores. *Clinical Oral Investigations*, **27**, 5813–5826.
- Al-Hiyali, A., Ayoub, A., Ju, X., Almuzian, M. and Al-Anezi, T. (2015) The impact of orthognathic surgery on facial expressions. *Journal of Oral and Maxillofacial Surgery*, **73**, 2380–2390.
- Bock, M. T. and Bowman, A. W. (2006) On the measurement and analysis of asymmetry with applications to facial modelling. *Journal of the Royal Statistical Society: Series C (Applied Statistics)*, **55**, 77–91.
- Boyett, J. M. and Shuster, J. J. (1977) Nonparametric one-sided tests in multivariate analysis with medical applications. *Journal of the American Statistical Association*, **72**, 665–668.
- Dryden, I. L. and Mardia, K. V. (2016) *Statistical Shape Analysis: With Applications in R*. Chichester: Wiley.
- Fisher, R. A. (1932) Statistical methods for research workers. In *Breakthroughs in Statistics: Methodology and Distribution* (eds. S. Kotz and N. L. Johnson), 66–70. Springer New York.
- Goodall, C. (1991) Procrustes methods in the statistical analysis of shape. with discussion. *Journal of the Royal Statistical Society: Series B (Methodological)*, **53**, 285–339.
- Kent, J. T. and Mardia, K. V. (2001) Shape, Procrustes tangent projections and bilateral symmetry. *Biometrika*, **88**, 469–485.

- Lehmann, E. and Romano, J. P. (2005) *Testing Statistical Hypotheses*. New York: Springer.
- Mann, H. B. and Whitney, D. R. (1947) On a test of whether one of two random variables is stochastically larger than the other. *The Annals of Mathematical Statistics*, **18**, 50–60.
- Mardia, K. V., Bookstein, F. L. and Moreton, I. J. (2000) Statistical assessment of bilateral symmetry of shapes. *Biometrika*, **87**, 285–300.
- Mardia, K. V., Kent, J. T. and Taylor, C. C. (2024) *Multivariate Analysis, Second Edition*. Chichester: John Wiley.
- Mardia, K. V. and Wu, X. (2025) On the distribution of weighted sum of two chi-squares with applications to shape analysis. *Sankhya Series A, a special issue: C. R. Rao, In Press*.
- Owen, A. B. (2009) Karl Pearson’s meta-analysis revisited. *The Annals of Statistics*, **37**, 3867–3892.
- Patel, Y., Sharp, I., Enocson, L. and Khambay, B. S. (2023) An innovative analysis of nasolabial dynamics of surgically managed adult patients with unilateral cleft lip and palate using 3D facial motion capture. *Journal of Plastic, Reconstructive and Aesthetic surgery*, **85**, 287–298.
- Pearson, K. (1934) On a new method of determining goodness of fit. *Biometrika*, **26**, 425–442.
- Quast, A., Sadlonova, M., Asendorf, T., Derad, C., Mouchoux, J., Horn, J., Schliephake, H., Kauffmann, P. and Meyer-Marcotty, P. (2023) The impact of orthodontic-surgical treatment on facial expressions—a four-dimensional clinical trial. *Clinical Oral Investigations*, **27**, 1–11.
- Stoyan, D. (1983) *Comparison Methods for Queues and Other Stochastic Models*. Wiley.
- Tukey, J. W. (1949) Comparing individual means in the analysis of variance. *Biometrics*, **5**, 99–114.
- Welch, B. L. (1947) The generalization of “Student’s” problem when several different population variances are involved. *Biometrika*, **34**, 28–35.

Weyl, H. (1952) *Symmetry*. Princeton University Press.

Xue, Z., Wu, L., Qiu, T., Li, Z., Wang, X. and Liu, X. (2020) Three-Dimensional Dynamic Analysis of the Facial Movement Symmetry of Skeletal Class III Patients With Facial Asymmetry. *Journal of oral and maxillofacial surgery : official journal of the American Association of Oral and Maxillofacial Surgeons*, **78**, 267–274.

Xue, Z., Ye, G., Qiu, T., Liu, X., Wang, X. and Li, Z. (2023) An objective, quantitative, dynamic assessment of facial movement symmetry changes after orthognathic surgery. *International Journal of Oral and Maxillofacial Surgery*, **52**, 272–281.